Advances in Radiation Oncology (2019) **4**, 79-89

advances
in radiation oncology

www.advancesradonc.org

Scientific Article

Percutaneous Image-Guided Nodal Biopsy After 11C-Choline PET/CT for Biochemically Recurrent Prostate Cancer: Imaging Predictors of Disease and Clinical Implications

Brian T. Welch MD [a,*], Ann T. Packard MD [a], Thomas D. Atwell MD [a], Geoffrey B. Johnson MD, PhD [a], Val J. Lowe MD [a], Robert Jeffrey Karnes MD [b], Lance A. Mynderse MD [b], Tina M. Gunderson MS [c], Sean S. Park MD [d], Bradley J. Stish MD [d], Jaden D. Evans MD [d], Eugene D. Kwon MD [b], Brian J. Davis MD, PhD [d], Mark A. Nathan MD [a]

Departments of [a]Radiology, [b]Urology, [c]Biostatistics, and [d]Radiation Oncology, Mayo Clinic, Rochester, Minnesota

Received 5 September 2017; revised 23 August 2018; accepted 27 August 2018

Abstract

Purpose: Management of recurrent prostate cancer necessitates timely diagnosis and accurate localization of the sites of recurrent disease. The purpose of this study was to assess predictors of histologic outcomes after 11C-choline positron emission tomography/computed tomography (CholPET) to increase the positive predictive value and specificity of CholPET in identifying imaging predictors of malignant and benign nodal disease to better inform clinical decision making regarding local therapy planning.

Materials and Methods: Retrospective review of patients undergoing CholPET followed by percutaneous core needle biopsy between January 1, 2010 and January 1, 2016. A total of 153 patients were identified who underwent 166 biopsy procedures. Patient, CholPET, procedural, and pathologic characteristics were recorded.

Results: A total of 157 biopsies were technically successful, and 110 (70.1%; 95% confidence interval, 62.2-77.1) yielded histologic results abnormal for metastatic prostate cancer. Lesion location, lesion maximum standardized uptake value (SUVmax), SUV ratio (calculated as the ratio of SUVmax to SUV mean in the right atrium), prostate-specific antigen, lesion short axis length, total Gleason score, and castration resistance were all associated with abnormal biopsy results (*P* values $<.001$, $<.001$, $<.001$, .02, .02, .02, and .015, respectively). External iliac, common iliac, and inguinal sites were associated with much lower rates of histologic positivity (mean [95% confidence interval], 51.2% [35.1-67.1], 46.2% [19.2-74.9], and 33.3% [7.5-70.1]), respectively.

Conclusions: In a cohort of patients in whom core needle biopsy was performed after CholPET,

Sources of support: This work had no specific funding.
Conflicts of interest: The authors have no conflicts of interest to disclose.

* Corresponding author. Department of Radiology, Mayo Clinic, 200 1st St SW, Rochester, MN 55905.
E-mail address: Welch.brian@mayo.edu (B.T. Welch).

https://doi.org/10.1016/j.adro.2018.08.022

characteristics of choline localization including node location, SUVmax, lesion–to–blood pool SUV ratio, prostate-specific antigen, total Gleason score, and castration resistance were significantly associated with abnormal biopsy results for metastatic disease on CholPET. Relatively high false positive rates were found in common iliac, external iliac, and inguinal lymph node locations. Histologic confirmation of these sites should be strongly considered in the appropriate clinical scenario before designing additional local therapy plans.

Introduction

Biochemical recurrence (BCR) after definitive therapy for prostate cancer (CaP) is common and represents a decision point in the management algorithm.[1,2] BCR has been reported in approximately 35% to 40% of men after radical prostatectomy or external beam radiation therapy.[3-7] Classification of BCR as local or systemic is vital to patient outcomes, with salvage treatment of locally recurrent disease associated with a 10-year cancer-specific survival of more than 70%.[8,9] Moreover, presumed systemic recurrence often results in initiation of long-term androgen deprivation therapy, which can diminish quality of life and may increase cardiovascular mortality.[10,11] Although predictive nomograms may be used to estimate the extent of prostate cancer recurrence,[9] to date, no biochemical assay has been validated in localizing recurrent CaP or distinguishing among local, regional, or systemic disease.

Advanced diagnostic imaging for CaP BCR recently was validated in accurate localization of disease recurrence. Specifically, multiparametric magnetic resonance imaging and 11C-choline positron emission tomography (PET)/computed tomography (CT) (CholPET) have provided independent and combined additive value in anatomic evaluation of BCR.[12-17] Moreover, a recent multivariate analysis documented that multiparametric magnetic resonance imaging and CholPET may provide a significant advantage over prior imaging methods, with increasing time from BCR to abnormal imaging independently associated with local-only disease recurrence.[16] Other PET agents, including Ga-68 prostate-specific membrane antigen and 18F-fluciclovine have had sensitivity similar or superior to that of 11C-choline and are of interest but are outside the scope of the present study.[18]

Because of recent advances in diagnostic imaging for BCR and the significant implications for accurate anatomic localization in treatment algorithms, percutaneous core needle biopsy (CNB) has become a common means for histologic confirmation of disease recurrence. No study to date has clearly elucidated patterns of nodal choline localization to allow accurate prediction of disease recurrence detected by CholPET, the locations of which have been described as "anatomically diverse."[16] Thus we analyzed the histologic results of patients undergoing percutaneous CNB of choline-avid lymph nodes after CholPET to assess imaging predictors of histologic outcomes, improve CholPET sensitivity, and better triage patients to biopsy or definitive treatment.

Materials and Methods

After institutional review board approval, a retrospective review of an institutionally maintained percutaneous image guided biopsy database and clinical data repository was undertaken to identify all patients who underwent CNB after CholPET for BCR between January 2010 and January 2016. Patients who underwent CholPET before initial prostate-directed therapy or biopsy based on physical examination or other imaging modalities were excluded from analysis. Additionally, patients who had an abnormal CholPET and a CNB yielding an entity other than CaP (eg, lymphoma) were excluded.

The previously published CholPET technique was performed according to the institutional standard clinical protocol.[1] Specifically, weight and height were recorded for all patients. CholPET studies (Discovery RX, 690, or 710; GE Healthcare) were performed after injection with 370 to 740 Mbq (mean dose 670 Mbq) of 11C-choline, and imaging began 5 minutes after injection. When possible, patients were imaged, with arms up, from orbits to midthighs using a 128 × 128 matrix and a rate of 3 minutes per bed position. PET images were reconstructed with a 3-dimensional ordered-subsets expectation maximization algorithm (28 subsets, 2 iterations). Low-dose helical CT images were obtained for attenuation correction and anatomic localization (detector row configuration, 16 · 0.625 mm; pitch, 1.75; gantry rotation time, 0.5 second; slice thickness, 3.75 mm; 140 kVP; and a range of 60-120 mAs using automatic current modulation). CT biopsy procedural guidelines have also been previously published.[19,20] A true positive was recorded for biopsy-proven nodal disease recurrence. See Figure 1 for an example of abnormal CholPET and subsequent biopsy.

Patient, procedural, and CholPET data were recorded for each patient. Specifically, lesions were classified by location as common iliac lymph node, deep pelvic lymph node,

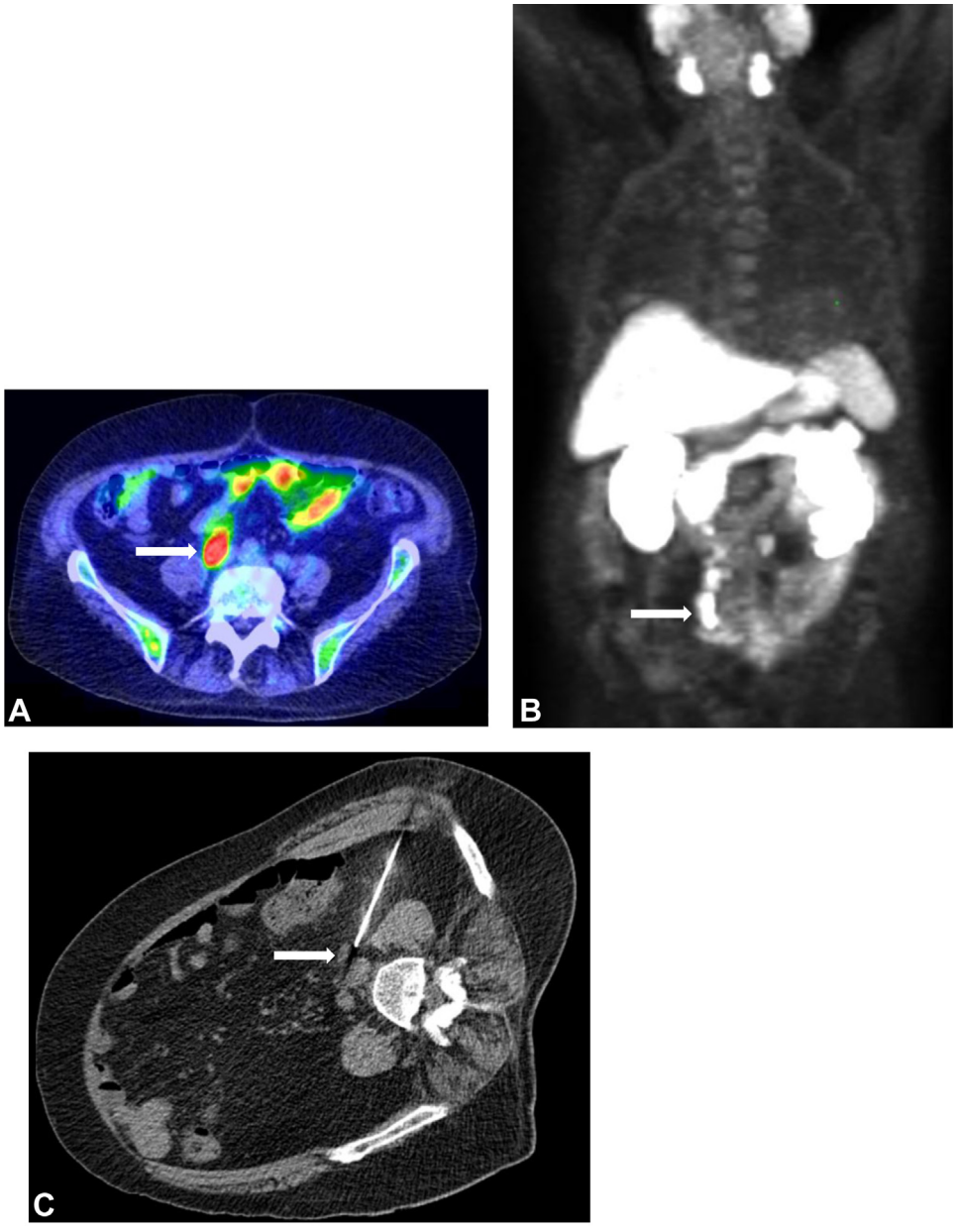

Figure 1 A 75-year-old man with Gleason 9 prostate cancer who had an elevated prostate-specific antigen (24.0 ng/dL) on androgen deprivation therapy. The biopsy results of the right common iliac lymph node identified metastatic prostate adenocarcinoma.

external iliac lymph node, retroperitoneal lymph node, inguinal lymph node, or other (supradiaphragmatic lymph node, pleural, or omental). The "other" biopsy site was used as a marker of advanced metastatic prostate cancer (mCaP). For each biopsy, lesion size and prostate-specific antigen (PSA) at the time of biopsy were recorded. Lesion maximum standardized uptake value (SUVmax) and SUV ratio (calculated as the ratio of SUVmax to SUV mean in the right atrial blood pool) were recorded from the index CholPET. Additional clinical information such as PSA nadir, PSA doubling time, testosterone, chromogranin A, total Gleason score, castration resistance, and hormone therapy at the time of examination was also obtained.

Descriptive statistics are provided as median and interquartile range or counts and percentages. Between-group comparisons used Kruskal-Wallis or Wilcoxon rank-sum tests for continuous variables and χ^2 tests for categorical variables. The proportion of abnormal results was calculated only on biopsies for which a sample was successfully obtained. Confidence intervals (CIs) for proportion of abnormal results were calculated using the Clopper-Pearson method. Sensitivity, specificity, positive predictive value, and negative predictive values were not provided given the small number of lesions per nodal basin and large CIs associated with these calculations. Classification prediction was performed via recursive

Table 1 Descriptive characteristics of biopsies with a choline PET scan

	Negative (N = 47)	Positive (N = 110)	Total (N = 157)	*P* value
Lesion Location				<.001
Common iliac	7 (14.9%)	6 (5.45%)	13 (8.28%)	
Deep pelvic	3 (6.38%)	41 (37.3%)	44 (28%)	
External iliac	20 (42.6%)	21 (19.1%)	41 (26.1%)	
Inguinal	6 (12.8%)	3 (2.73%)	9 (5.73%)	
Other	4 (8.51%)	23 (20.9%)	27 (17.2%)	
Retroperitoneal	7 (14.9%)	16 (14.5%)	23 (14.6%)	
Blood pool SUV mean				.100
Median (IQR)	1.25 (1.06, 1.45)	1.16 (0.98, 1.38)	1.19 (0.99, 1.39)	
Lesion SUV maximum				<.001
Median (IQR)	2.93 (2.13, 4.34)	4.19 (2.9, 5.7)	3.94 (2.73, 5.21)	
SUV ratio				<.001
Median (IQR)	2.45 (1.72, 3.38)	3.81 (2.29, 5.39)	3.25 (2.11, 4.79)	
Long axis length (mm)				.125
Median (IQR)	12 (10, 14.5)	13 (9.25, 19)	13 (10, 17)	
Short axis length (mm)				.017
Median (IQR)	9 (7, 11)	10 (8, 15.8)	10 (8, 14)	
PSA at exam (ng/mL)				.023
Median (IQR)	2 (0.945, 5.1)	3.4 (1.42, 7.77)	3.1 (1.1, 7.3)	
Nadir PSA				.962
Median (IQR)	0.15 (0.05, 0.5)	0.1 (0.05, 0.73)	0.11 (0.05, 0.67)	
PSA doubling time				.374
Median (IQR)	3.5 (2.5, 7.97)	4.7 (2.8, 9.8)	4.7 (2.6, 9.8)	
Testosterone				.668
Median (IQR)	274 (11.6, 403)	274 (5.5, 394)	274 (7.8, 404)	
Chromagranin A				.917
Median (IQR)	83 (53, 120)	90 (56, 192)	84.5 (53.8, 171)	
Total Gleason score				.021
Median (IQR)	7 (7, 8)	7 (7, 9)	7 (7, 9)	
Castration resistant				.015
N	42 (91.3%)	77 (72%)	119 (77.8%)	
Y	4 (8.7%)	30 (28%)	34 (22.2%)	
Lymph node positivity				.278
N-Miss	10	18	28	
N	33 (91.7%)	73 (82%)	106 (84.8%)	
Y	3 (8.33%)	16 (18%)	19 (15.2%)	
Therapy				.062
HORMONE	8 (17.4%)	35 (32.7%)	43 (28.1%)	
HORMONE+CHEMO	0 (0%)	4 (3.74%)	4 (2.61%)	
HORMONE+IT	0 (0%)	2 (1.87%)	2 (1.31%)	
None	38 (82.6%)	66 (61.7%)	104 (68%)	

Abbreviations: CHEMO = Chemotherapy; HORMONE = Hormonal therapy; IQR = interquartile range; IT = Immunotherapy; PET = positron emission tomography; PSA = prostate-specific antigen; SUV = standardized uptake value.

partitioning. Degree of tree complexity was selected to minimize cross-validated relative error. Potential predictors included location of lesion, PSA, lesion minimum and maximum size, SUVmax of the lesion, SUV mean of blood pool, SUV ratio (defined as lesion SUVmax / blood pool SUVmean), PSA nadir, PSA doubling time, testosterone, chromogranin A, total Gleason score, castration resistance, and hormone therapy at the time of examination. Although recursive partitioning was selected to increase result interpretability, gradient boosting machine models were also built to compare variable importance estimation. *P* values less than .05 were considered significant. Statistical analysis was performed in R (version 3.2.3; R Foundation for Statistical Computing, Vienna, Austria; rpart version 4.1-10; rpart.plot version 2.1.0).

Results

A total of 166 total biopsies were performed in 153 unique patients after CholPET. Nine biopsies (5%) were classified as technical failures based on inadequate or nondiagnostic tissue sampling. Of the 157 technically

successful biopsies, 110 (70%; 95% CI, 62.2-77.1) yielded pathologic results indicative of mCaP. Forty-seven biopsies were technically successful but were negative for mCaP. The most common biopsy sites were deep pelvic nodes (n = 44) and external iliac nodes (n = 41). Characteristics of the full patient cohort by biopsy outcomes are summarized in Table 1. Specifically, lesion location, lesion SUVmax, SUV ratio, PSA, lesion short axis length, total Gleason score, and castration resistance were all associated with abnormal biopsy results with statistical significance (*P* values <.001, <.001, <.001, .023, .017, .02, and .015, respectively). The recursive partitioning model is shown in Figure 2. The most important variables for predicting a abnormal biopsy outcome were lesion location, SUV ratio, and PSA value in both recursive partitioning and GBM models. Deep pelvic nodes and retroperitoneal and other biopsy locations were strongly associated with an abnormal biopsy result. All biopsy sites with a PSA greater than 6.9 were likely to be abnormal at biopsy.

Site-specific biopsy characteristics are summarized in Table 2. No significant differences among biopsy sites were present for lesion SUVmax, SUV ratio, lesion short axis length, or PSA. Long axis length was significantly higher for lesions in the inguinal lymph nodes (Table 2). The proportion of abnormal biopsy results by location is summarized in Table 3. A total of 41 of 44 deep pelvic (93%; 95% CI, 0.81-0.98) nodal biopsy results were abnormal. External iliac, common iliac, and inguinal sites were associated with much lower rates of histologic abnormality (mean [95% CI], 51.2% [35.1-67.1], 46.2% [19.2-74.9], and 33.3% [7.5-70.1]). Figure 3 demonstrates rates of abnormal biopsy for choline avid lymph nodes by anatomic nodal basin.

To identify CholPET predictors of normal histologic outcomes, a site-specific analysis stratified by biopsy outcome was completed (Table 4). External iliac nodes were the most common site of normal biopsy result (20/41, 49%). External iliac nodes with a normal histologic outcome had statistically significant lower PSA values (median [interquartile range], 2.1 [0.8-4.4] vs 7.7 [5.0-12.6]) and SUV ratios (2.2 [1.7-3.1] vs 4.2 [3.4-5.6]) (Table 4). Inguinal lymph nodes were also commonly associated with normal histologic outcomes (6/9, 67%) with SUV ratios significantly lower in the cohort who had normal biopsy results.

Discussion

Our study found that CholPET was associated with acceptable positive predictive value for detection of mCaP in a select cohort of patients who underwent CNB to achieve histologic confirmation of disease. Moreover, our results suggest CholPET sensitivity can be further enhanced based on several factors. Specifically, lesion location, SUVmax, lesion–to–blood pool SUV ratio, total Gleason score, and castration resistance are significantly associated

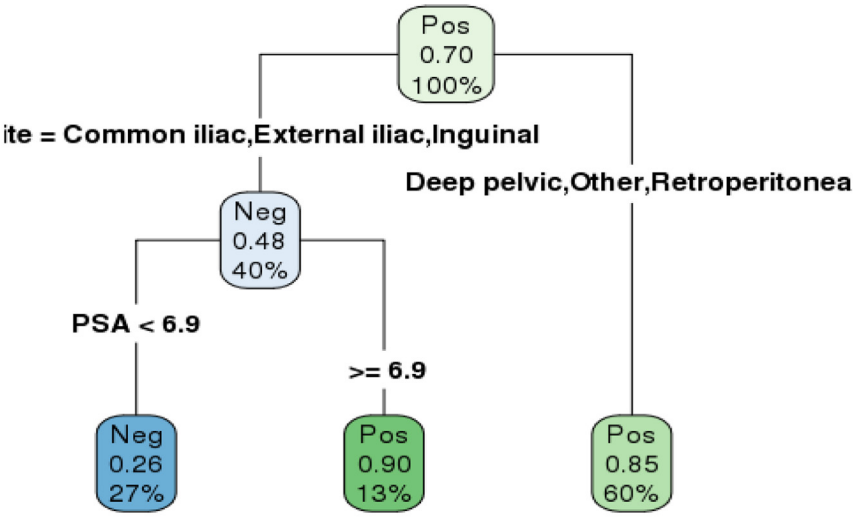

Comparison of model prediction results to observed results.

	Observed	
Predicted	Neg	Pos
Neg	31	11
Pos	16	99

Figure 2 Recursive partitioning plot for choline data. Each circle on represents the predicted class, the predicted probability of an abnormal result, and the percentage of observations that group. *Abbreviations:* Neg = negative; Pos = positive; PSA = prostate-specific antigen.

Table 2 Comparison of biopsy characteristics by site of biopsy

	Common iliac (N = 13)	Deep pelvic (N = 44)	External iliac (N = 41)	Inguinal (N = 9)	Other (N = 27)	Retroperitoneal (N = 23)	Total (N = 157)	*P* value
Blood pool SUV mean								.945
Median (IQR)	1.18 (0.96, 1.31)	1.21 (1.05, 1.42)	1.19 (0.93, 1.45)	1.28 (0.98, 1.3)	1.19 (1.04, 1.39)	1.16 (0.985, 1.36)	1.19 (0.99, 1.39)	
Lesion SUV maximum								.734
Median (IQR)	4.48 (2.51, 5.28)	3.69 (2.56, 4.6)	3.54 (2.74, 5.52)	4.26 (3.23, 5.63)	4.2 (3.5, 5.74)	3.82 (2.74, 5)	3.94 (2.73, 5.21)	
SUV ratio								.589
Median (IQR)	3.34 (2.34, 5.5)	2.89 (1.94, 4.08)	3.36 (2.12, 4.53)	4.4 (2.51, 5.3)	3.7 (2.72, 5.57)	2.85 (2.3, 4.98)	3.25 (2.11, 4.79)	
Long axis length (mm)								.039
Median (IQR)	11 (9, 14)	12 (9, 16)	13 (10, 17)	18 (15, 23)	15 (12, 23)	11 (9.5, 14.5)	13 (10, 17)	
Short axis length (mm)								.279
Median (IQR)	10 (8, 11)	9 (8, 14)	9 (8, 14)	11 (8, 13)	12 (8.5, 20)	8 (7, 11)	10 (8, 14)	
PSA (ng/mL)								.433
Median (IQR)	3.4 (1.1, 4.9)	1.95 (1.3, 3.83)	5 (1.8, 7.8)	3.4 (2.1, 7.5)	3.6 (1, 14)	3.2 (1.1, 8.15)	3.1 (1.1, 7.3)	
Positive biopsy								<.001
No	7 (53.8%)	3 (6.82%)	20 (48.8%)	6 (66.7%)	4 (14.8%)	7 (30.4%)	47 (29.9%)	
Yes	6 (46.2%)	41 (93.2%)	21 (51.2%)	3 (33.3%)	23 (85.2%)	16 (69.6%)	110 (70.1%)	

Abbreviations: IQR = interquartile range; PSA = prostate-specific antigen; SUV = standardized uptake value.

with an abnormal histologic outcome after CNB. Lesion location is an important independent predictor of histologic outcome, with deep pelvic nodes, retroperitoneal nodes, and other biopsy groups being abnormal on 85% of CNBs (Fig 2). The recursive partitioning analysis shown in Figure 2 provides information that may be useful to clinicians in discussing the chances of abnormal biopsy results with a patient and interventionalist as part of the shared decision-making process. Moreover, common iliac, external iliac and inguinal lymph nodes were associated with high rates of false positive CholPET.

These data are clinically relevant particularly when considering salvage radiation therapy to lymph nodes in patients who experience BCR.[9,21,22] The data presented herein provide a histologic correlation to commonly observed CholPET-avid sites of recurrence and confirm our understanding of high-risk nodal basins where disease recurs, such as deep pelvic lymph nodes including internal iliac and obturator nodal basins. Furthermore, the data provide insight into nodal basins where the probability of a false positive is relatively high, such as common iliac, external iliac, and inguinal lymph nodal basins. The design of pelvic radiation therapy fields is nonstandard across clinical trials or published guidelines,[23] and recent data indicating patterns of recurrence postprostatectomy, post–definitive radiation therapy, and post–prostatectomy radiation therapy have highlighted how advanced imaging may be used to more effectively design plans for additional local therapy.[9,16,21] However, our analysis provides some reason for pause in relying entirely on the radiographic findings to guide clinical practice and radiation field design, particularly when the CholPET-avid site occurs in a known region of high false positivity, such as the common iliac, external iliac, or inguinal lymph nodes.

Table 3 Point estimate and 95% Clopper-Pearson confidence intervals for proportion of successful biopsies, both overall and by biopsy site

Location	Negative biopsies	Positive biopsies	Total biopsies	Mean	Lower 95% CI	Upper 95% CI
Common iliac	7	6	13	0.462	0.192	0.749
Deep pelvic	3	41	44	0.932	0.813	0.986
External iliac	20	21	41	0.512	0.351	0.671
Inguinal	6	3	9	0.333	0.075	0.701
Other	4	23	27	0.852	0.663	0.958
Retroperitoneal	7	16	23	0.696	0.471	0.868
All	47	110	157	0.701	0.622	0.771

Abbreviation: CI = confidence interval.

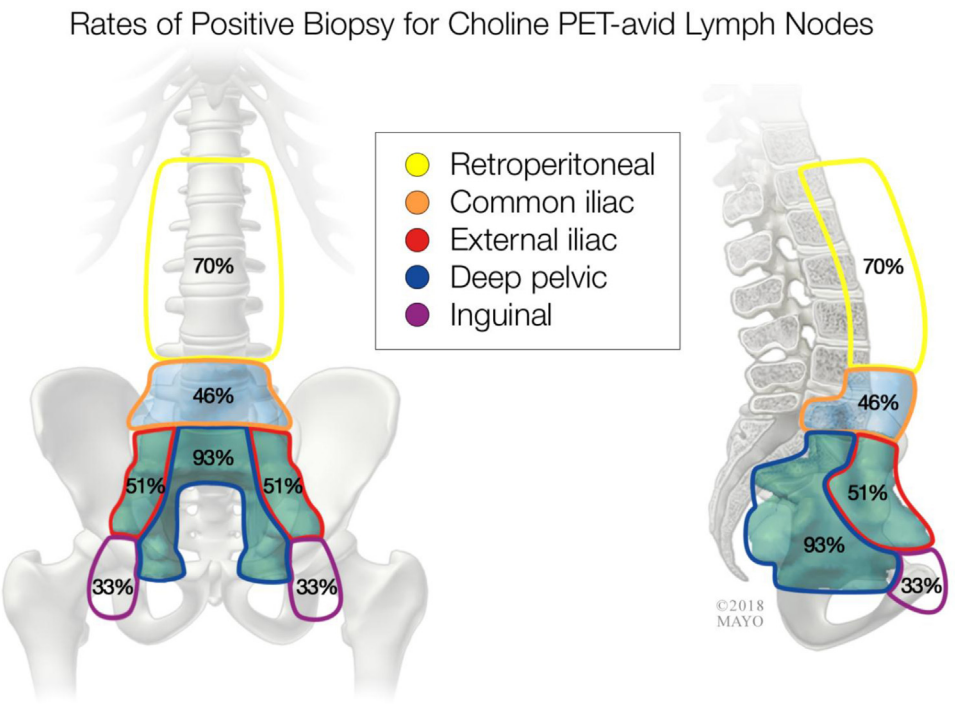

Figure 3 Anatomic delineation of rates of abnormal biopsy results for choline avid lymph nodes by nodal basin.

Given the relatively high false positive rate in the common iliac, external iliac, and inguinal lymph nodal basins, histologic confirmation may be more important when clinical decision making depends on these sites. No present guideline recommends routine coverage of inguinal lymph nodes in elective pelvic radiation therapy design. Given the low positive rate of inguinal lymph node involvement in this series, no change in current management is suggested. Nevertheless, abnormal inguinal lymph nodes are identified and confirmed by CNB in one-third of patients with CholPET. Therefore such a radiographic finding (asymmetrically enlarged with considerable choline uptake) is important, and given the relative ease of inguinal node biopsy, a decision to initiate CNB in PET-avid inguinal lymph nodes is not unreasonable because the findings could affect subsequent management.

There are a number of reasons why examining histologic outcomes after CholPET is important. Much debate has focused on the sensitivity of CholPET in detection of BCR CaP. Several studies have documented overall sensitivity and specificity of CholPET between 86% to 100% and 76% to 96%, respectively.[1,2,9,13,16,24,25] Other studies have reported lower sensitivity of CholPET with per-patient sensitivity of approximately 60% and a 20% false positive rate.[26,27] The relatively lower sensitivity of CholPET in our study is likely related to a combination of heterogeneity in initial treatment strategy and, most importantly, the exclusion of cases for which histologic confirmation was not pursued because of very strong imaging and/or clinical indicators of recurrent CaP. For example, Giovacchini et al[13] previously described a PSA threshold of 1.4 ng/mL in predicting positive and negative CholPET. Many of the previous studies describing CholPET sensitivity have 11% to 59% rates of histologic confirmation.[9,13,16] Moreover, the intent of this study was not to report the overall sensitivity or predictive value of CholPET but to identify which clinical and CholPET imaging characteristics significantly predict abnormal histologic results such that patients can be more appropriately triaged for CNB.

Our results suggest that deep pelvic lymph nodes with a high SUV ratio (>3.2) are strongly associated with positive histologic outcomes, and the need for biopsy may be obviated. Additionally, common iliac, external iliac, and inguinal lymph nodes were commonly associated with normal histologic outcomes. External iliac and inguinal nodes without highly suspicious, marked focal elevation in choline activity (SUV ratio >4.2 and 7.4, respectively) or associated PSA elevation to suggest recurrence are associated with normal histologic outcomes, and the need for biopsy may be obviated. No inguinal lymph node with an SUV ratio < 4.6 was positive for mCaP in this patient cohort. Common iliac and retroperitoneal nodes were associated with heterogeneous histologic outcomes, and there was no statistically significant differentiation based on SUV, SUV ratio, or PSA. These nodal locations may benefit from histologic sampling to achieve confirmation of mCaP. Clinical characteristics such as castrateion resistance, PSA at time of examination, and Gleason score are secondary markers for aggressive or advanced CaP and were all associated with abnormal histologic outcomes.

Table 4 Descriptive statistics by site

Deep pelvic	Negative	Positive	Total	*P* value
	N = 3	N = 41	N = 44	
Blood Pool SUV Mean				.376
Median (IQR)	1.33 (1.25, 1.46)	1.21 (1.04, 1.41)	1.21 (1.05, 1.42)	
Range	1.18-1.59	0.76-2.07	0.76-2.07	
Lesion SUV Maximum				.217
Median (IQR)	2.05 (1.98, 3.12)	3.86 (2.69, 4.64)	3.69 (2.56, 4.6)	
Range	1.91-4.19	1.21-10.6	1.21-10.6	
SUV ratio				.098
Median (IQR)	1.74 (1.59, 2.19)	3.17 (1.99, 4.13)	2.89 (1.94, 4.08)	
Range	1.44-2.64	0.985-9.25	0.985-9.25	
Long axis length (mm)				.591
Median (IQR)	14 (12, 15)	12 (9, 16)	12 (9, 16)	
Range	10-16	7-39	7-39	
Short axis length (mm)				.925
Median (IQR)	11 (9, 12.5)	9 (8, 14)	9 (8, 14)	
Range	7-14	5-38	5-38	
PSA (ng/mL)				.625
Median (IQR)	0.95 (0.85, 9.62)	2 (1.3, 3.6)	1.95 (1.3, 3.83)	
Range	0.75-18.3	0.1-34	0.1-34	
External iliac	N = 20	N = 21	N = 41	
Blood Pool SUV Mean				.070
Median (IQR)	1.21 (1.13, 1.51)	1.11 (0.92, 1.24)	1.19 (0.93, 1.45)	
Range	0.77-1.85	0.4-1.59	0.4-1.85	
Lesion SUV Maximum				.001
Median (IQR)	2.76 (2.4, 3.4)	4.75 (3.54, 6.61)	3.54 (2.74, 5.52)	
Range	0.89-8.47	2.02-8.74	0.89-8.74	
SUV ratio				<.001
Median (IQR)	2.23 (1.74, 3.14)	4.2 (3.41, 5.56)	3.36 (2.12, 4.53)	
Range	1.03-5.84	1.54-18.3	1.03-18.3	
Long axis length (mm)				.277
Median (IQR)	12 (10, 14.8)	16 (9, 22)	13 (10, 17)	
Range	6-29	8-61	6-61	
Short axis length (mm)				.018
Median (IQR)	9 (7, 10.2)	13 (9, 16)	9 (8, 14)	
Range	4-28	6-40	4-40	
PSA (ng/mL)				<.001
Median (IQR)	2.05 (0.815, 4.4)	7.7 (5, 12.6)	5 (1.8, 7.8)	
Range	0.1-8.8	0.49-256	0.1-256	
Inguinal	N = 6	N = 3	N = 9	
Blood Pool SUV Mean				.364
Median (IQR)	1.29 (1.12, 1.43)	0.98 (0.95, 1.14)	1.28 (0.98, 1.3)	
Range	0.61-1.79	0.92-1.3	0.61-1.79	
Lesion SUV Maximum				.071
Median (IQR)	3.62 (2.38, 4.38)	7.36 (5.81, 8.5)	4.26 (3.23, 5.63)	
Range	1.62-5.63	4.26-9.63	1.62-9.63	
SUV ratio				.039
Median (IQR)	2.62 (1.83, 3.98)	7.41 (6.02, 7.46)	4.4 (2.51, 5.3)	
Range	1.53-5.3	4.63-7.51	1.53-7.51	
Long axis length (mm)				.302
Median (IQR)	16.5 (13.5, 21.8)	20 (18.5, 24.5)	18 (15, 23)	
Range	10-26	17-29	10-29	
Short axis length (mm)				.195
Median (IQR)	9 (8, 12.2)	12 (11.5, 19.5)	11 (8, 13)	
Range	7-14	11-27	7-27	

(*continued on next page*)

Table 4 (*continued*)

Inguinal	N = 6	N = 3	N = 9	
PSA (ng/mL)				.071
Median (IQR)	2.3 (2.02, 3.17)	7.5 (7.3, 9.6)	3.4 (2.1, 7.5)	
Range	0.37-8.6	7.1-11.7	0.37-11.7	
Common iliac	N = 7	N = 6	N = 13	
Blood Pool SUV Mean				.474
Median (IQR)	1.25 (1.17, 1.29)	1.05 (0.952, 1.29)	1.18 (0.96, 1.31)	
Range	0.94-1.51	0.89-1.51	0.89-1.51	
Lesion SUV Maximum				.391
Median (IQR)	4.48 (2.48, 4.83)	4.12 (2.62, 6.54)	4.48 (2.51, 5.28)	
Range	1.57-6.94	2.35-13.2	1.57-13.2	
SUV ratio				.475
Median (IQR)	3.34 (2.03, 3.52)	4.41 (2.68, 5.91)	3.34 (2.34, 5.5)	
Range	1.67-6.03	1.66-9.81	1.66-9.81	
Long axis length (mm)				.246
Median (IQR)	10 (9, 12.5)	12.5 (10.5, 15.2)	11 (9, 14)	
Range	9-15	9-18	9-18	
Short axis length (mm)				.884
Median (IQR)	10 (7, 11.5)	10 (9.25, 10)	10 (8, 11)	
Range	5-13	8-12	5-13	
PSA (ng/mL)				.086
Median (IQR)	1.1 (0.51, 3.4)	4.1 (3.55, 9.53)	3.4 (1.1, 4.9)	
Range	0.1-5.3	1.2-21	0.1-21	
Other	N = 4	N = 23	N = 27	
Blood Pool SUV Mean				.707
Median (IQR)	1.17 (1.04, 1.3)	1.19 (1.02, 1.44)	1.19 (1.04, 1.39)	
Range	1.04-1.31	0.7-1.96	0.7-1.96	
Lesion SUV Maximum				.495
Median (IQR)	3.63 (3.55, 4.2)	4.2 (3.41, 6.05)	4.2 (3.5, 5.74)	
Range	3.42-5.74	1-11.7	1-11.7	
SUV ratio				.585
Median (IQR)	3.13 (2.76, 3.97)	3.97 (2.53, 5.71)	3.7 (2.72, 5.57)	
Range	2.63-5.52	0.546-7.34	0.546-7.34	
Long axis length (mm)				.707
Median (IQR)	13 (12, 19.5)	15 (11, 23)	15 (12, 23)	
Range	12-36	8-58	8-58	
Short axis length (mm)				.392
Median (IQR)	15.5 (13, 17.8)	10 (8, 21)	12 (8.5, 20)	
Range	10-20	6-44	6-44	
PSA (ng/mL)				.608
Median (IQR)	3.05 (0.958, 5.05)	3.6 (1, 20.6)	3.6 (1, 14)	
Range	0.53-5.2	0.1-256	0.1-256	
Retroperitoneal	N = 7	N = 16	N = 23	
Blood Pool SUV Mean				.462
Median (IQR)	1.12 (1.06, 1.37)	1.16 (0.975, 1.27)	1.16 (0.985, 1.36)	
Range	0.97-2.08	0.84-1.68	0.84-2.08	
Lesion SUV Maximum				.061
Median (IQR)	2.74 (2.12, 3.75)	4.14 (2.9, 5.82)	3.82 (2.74, 5)	
Range	1.77-5.08	2.2-17.9	1.77-17.9	
SUV ratio				.095
Median (IQR)	2.45 (1.76, 3.04)	3.88 (2.44, 5.48)	2.85 (2.3, 4.98)	
Range	1-4.79	1.69-18.7	1-18.7	
Long axis length (mm)				.029
Median (IQR)	9 (7.5, 11.5)	12 (10, 19.5)	11 (9.5, 14.5)	
Range	6-13	8-41	6-41	

(*continued on next page*)

Table 4 (*continued*)

Retroperitoneal	N = 7	N = 16	N = 23	
Short axis length (mm)				.046
Median (IQR)	7 (6.5, 8)	9.5 (7, 13.5)	8 (7, 11)	
Range	5-10	6-24	5-24	
PSA (ng/mL)				.738
Median (IQR)	5.7 (1.1, 9.05)	2.9 (1.2, 7.1)	3.2 (1.1, 8.15)	
Range	1-10.2	0.11-35	0.11-35	

Abbreviations: IQR = interquartile range; PSA = prostate-specific antigen; SUV = standardized uptake value.

Our study has several limitations. First, the study is retrospective in nature and occurred over an extended period with expected evolution in CholPET technique and interpreter experience. The cohort of patients is relatively heterogeneous in initial treatment strategy and therapies used before CNB, which introduces selection bias. Only participants who received both a CholPET and subsequent CNB are included in the cohort. Patients who were treated for mCaP without histologic confirmation via CNB were excluded. Because of considerations for ease of interpretation and implementation, recursive partitioning was used instead of a more complex model such as gradient boosting machines (GBM). Although additional analysis was performed to compare relative variable importance between GBM and recursive partitioning models, more complicated models such as GBM or random forest nevertheless are more robust and could potentially provide better classification.

Conclusions

In a cohort of patients in whom CNB was performed after CholPET, characteristics of choline localization including lesion location, SUVmax, and lesion−to−blood pool SUV ratio were significantly associated with identification of metastatic disease on CholPET. Relatively high false positive rates were identified in common iliac, external iliac, and inguinal lymph node locations. Histologic confirmation of these sites should be strongly considered in the appropriate clinical scenario before designing additional local therapy plans. Deep pelvic lymph nodes were overwhelmingly associated with abnormal histologic results.

References

1. Mitchell CR, Lowe VJ, Rangel LJ, et al. Operational characteristics of (11)c-choline positron emission tomography/computerized tomography for prostate cancer with biochemical recurrence after initial treatment. *J Urol*. 2013;189:1308-1313.
2. Mohler JL, Armstrong AJ, Bahnson RR, et al. Prostate Cancer, Version 1.2016. *J Natl Compr Canc Netw*. 2016;14:19-30.
3. Khuntia D, Reddy CA, Mahadevan A, Klein EA, Kupelian PA. Recurrence-free survival rates after external-beam radiotherapy for patients with clinical T1-T3 prostate carcinoma in the prostate-specific antigen era: What should we expect? *Cancer*. 2004; 100:1283-1292.
4. Roehl KA, Han M, Ramos CG, Antenor JA, Catalona WJ. Cancer progression and survival rates following anatomical radical retropubic prostatectomy in 3,478 consecutive patients: Long-term results. *J Urol*. 2004;172:910-914.
5. Rosser CJ, Chichakli R, Levy LB, Kuban DA, Smith LG, Pisters LL. Biochemical disease-free survival in men younger than 60 years with prostate cancer treated with external beam radiation. *J Urol*. 2002;168:536-541.
6. Sandler HM, Dunn RL, McLaughlin PW, et al. Overall survival after prostate-specific-antigen-detected recurrence following conformal radiation therapy. *Int J Radiat Oncol Biol Phys*. 2000;48:629-633.
7. Ward JF, Blute ML, Slezak J, Bergstralh EJ, Zincke H. The long-term clinical impact of biochemical recurrence of prostate cancer 5 or more years after radical prostatectomy. *J Urol*. 2003;170:1872-1876.
8. Chade DC, Eastham J, Graefen M, et al. Cancer control and functional outcomes of salvage radical prostatectomy for radiation-recurrent prostate cancer: A systematic review of the literature. *Eur Urol*. 2012;61:961-971.
9. Parker WP, Davis BJ, Park SS, et al. Identification of site-specific recurrence following primary radiation therapy for prostate cancer using 11C-choline positron emission tomography/computed tomography: A nomogram for predicting extrapelvic disease. *Eur Urol*. 2016;71:340-348.
10. Alibhai SM, Breunis H, Timilshina N, et al. Long-term impact of androgen-deprivation therapy on physical function and quality of life. *Cancer*. 2015;121:2350-2357.
11. Taylor LG, Canfield SE, Du XL. Review of major adverse effects of androgen-deprivation therapy in men with prostate cancer. *Cancer*. 2009;115:2388-2399.
12. Giovacchini G, Incerti E, Mapelli P, et al. [^{11}C]Choline PET/CT predicts survival in hormone-naive prostate cancer patients with biochemical failure after radical prostatectomy. *Eur J Nucl Med Mol Imaging*. 2015;42:877-884.
13. Giovacchini G, Picchio M, Coradeschi E, et al. Predictive factors of [(11)C]choline PET/CT in patients with biochemical failure after radical prostatectomy. *Eur J Nucl Med Mol Imaging*. 2010;37:301-309.
14. Hernandez D, Salas D, Gimenez D, et al. Pelvic MRI findings in relapsed prostate cancer after radical prostatectomy. *Radiat Oncol*. 2015;10:262.
15. Linder BJ, Kawashima A, Woodrum DA, et al. Early localization of recurrent prostate cancer after prostatectomy by endorectal coil magnetic resonance imaging. *Can J Irol*. 2014;21:7283-7289.
16. Sobol I, Zaid HB, Haloi R, et al. Contemporary mapping of post-prostatectomy prostate cancer relapse with 11C-choline PET and multiparametric MRI. *J Urol*. 2017;197:129-134.
17. Zattoni F, Kawashima A, Morlacco A, et al. Detection of recurrent prostate cancer after primary radiation therapy: An evaluation of the role of multiparametric 3T magnetic resonance imaging with endorectal coil. *Pract Radiat Oncol*. 2016;7:42-49.

18. Hofman MS, Hicks RJ, Maurer T, Eiber M. Prostate-specific membrane antigen PET: Clinical utility in prostate cancer, normal patterns, pearls, and pitfalls. *Radiographics*. 2018;38:200-217.
19. Atwell TD, Smith RL, Hesley GK, et al. Incidence of bleeding after 15,181 percutaneous biopsies and the role of aspirin. *AJR Am J Roentgenol*. 2010;194:784-789.
20. Atwell TD, Spanbauer JC, McMenomy BP, et al. The timing and presentation of major hemorrhage after 18,947 image-guided percutaneous biopsies. *AJR Am J Roentgenol*. 2015;205:190-195.
21. Parker WP, Evans JD, Stish BJ, et al. Patterns of recurrence after postprostatectomy fossa radiation therapy identified by 11C-choline positron emission tomography/computed tomography. *Int J Radiat Oncol Biol Phys*. 2017;97:526-535.
22. Picchio M, Berardi G, Fodor A, et al. (11)C-Choline PET/CT as a guide to radiation treatment planning of lymph-node relapses in prostate cancer patients. *Eur J Nucl Med Mol Imaging*. 2014;41:1270-1279.
23. Harris VA, Staffurth J, Naismith O, et al. Consensus guidelines and contouring atlas for pelvic node delineation in prostate and pelvic node intensity modulated radiation therapy. *Int J Radiat Oncol Biol Phys*. 2015;92:874-883.
24. Kitajima K, Murphy RC, Nathan MA, et al. Detection of recurrent prostate cancer after radical prostatectomy: Comparison of 11C-choline PET/CT with pelvic multiparametric MR imaging with endorectal coil. *J Nucl Med*. 2014;55:223-232.
25. Umbehr MH, Müntener M, Hany T, Sulser T, Bachmann LM. The role of 11C-choline and 18F-fluorocholine positron emission tomography (PET) and PET/CT in prostate cancer: A systematic review and meta-analysis. *Eur Urol*. 2013;64:106-117.
26. Bossi A, Mottet N, Blanchard P. Choline positron emission tomography/computed tomography for selection of patients for salvage strategies after primary local treatment of prostate cancer and rising prostate-specific antigen: Ready for prime time? *Eur Urol*. 2017;71:349-350.
27. Ploussard G, Almeras C, Briganti A, et al. Management of node only recurrence after primary local treatment for prostate cancer: A systematic review of the literature. *J Urol*. 2015;194:983-988.